

\mathcal{L}_1 ADAPTIVE CONTROLLER DESIGN FOR GUST LOAD ALLEVIATION

Elisa Capello*, Giorgio Guglieri*, Fulvia Quagliotti*

***Politecnico di Torino, Department of Mechanical and Aerospace Engineering,
Corso Duca degli Abruzzi 24, 10129 Torino, Italy**

Keywords: *Adaptive Controller, Gust Load Alleviation, Flexible Aircraft*

Abstract

The objective of this paper is the implementation and validation of an adaptive controller for gust load alleviation. The main contribution of this research is the design of a robust controller that guarantees the reduction of the gust loads, even when the nominal conditions change. Some preliminary results are presented, considering the symmetric aileron deflection as control device. The proposed approach is validated on a subsonic transport aircraft for different mass and flight conditions: even when the gust frequency changes, no parameter retuning is required.

1. Introduction

Gust load alleviation systems are usually used to reduce the airframe loads and to improve passenger comfort. Active control techniques for gust load alleviation have been investigated extensively in the last years to control the aeroelastic response and to improve the handling qualities of the aircraft. Different approaches have been developed for gust alleviation and load control, including design of classical robust controllers, such as the linear quadratic regulator [1] and gaussian theories [2], model predictive control algorithms [3], H_∞ robust control [4], [5].

Because of time varying characteristics of the aircraft dynamics, it is difficult to synthesize a *unique control* law for the whole flight envelope and a gain scheduling should be required to account for the time varying dynamics. For this reason, adaptive feedback and/or feedforward controllers have been considered for adverse situations

due to their ability of modify a pre-existing control design.

The objective of the present paper is to derive a controller that is robust in the presence of model uncertainties, due to weight and flight condition variations. Moreover, the present paper aims at proposing an application of \mathcal{L}_1 adaptive control techniques in the framework of flexible fixed wing subsonic aircraft, stabilizing the system under different operating conditions and when different gusts occur.

Some classical controllers, as H_∞ application, have limitations in terms of frequency band (only low frequencies are analyzed) and no uncertainties or variations on the nominal parameters are considered, as in the works of [4], [6]. Recently, Jansson and Eller [5] included uncertainties in the model parameters but the gust is included as a Gaussian white noise of unit intensity and zero mean, that is not a realistic case. In [7] two uncertainty models to decide what flexible modes to be truncated from the original flexible system model while preserving closed-loop performance are presented. Robust control framework is used with the robust performance criterion to show that the new inverse uncertainty representation of flexible modes gives good closed-loop performance, but this controller is not validated with different mass and flight conditions.

To overcome these limitations adaptive feedback [8], [9] and feedforward controllers [10], [11] are implemented. Wildschek [12] proposed an adaptive Multi Input - Multi Output (MIMO) feedforward controller and a feedback H_2 controller. No uncertainties are considered and the adaptive controller alleviated only the wing bending accel-

eration.

\mathcal{L}_1 adaptive control theory reduces the tuning effort required to achieve desired closed-loop performance, particularly while operating in the presence of uncertainties and failures. The adaptive law is a piecewise constant law, that guarantees fast estimation, and the adaptation rate can be associated with the sampling rate of the onboard CPU. Moreover, this adaptive algorithm guarantees bounded inputs and outputs, uniform transient response and steady-state tracking.

The paper is organized as follows. In Section 2 the aircraft model description and formulation is presented. In the same Section the gust and load models are described. In Section 3 the actuator models are analyzed. In Section 4 the control architecture of the \mathcal{L}_1 controller is introduced. The controller design and the simulation results are described in Section 5. Conclusions are summarized in Section 6.

2. Aircraft and Gust Mathematical Model

For the implementation of the proposed feedback controller only the longitudinal plane of a subsonic transport aircraft is considered. For the mathematical formulation of the dynamic system a standard continuous time-invariant state space formulation

$$\begin{aligned} \dot{x}(t) &= Ax(t) + Bu(t) + B_g w_g(t), \\ y(t) &= Cx(t) + D_g w_g(t), \quad x(0) = x_0, \end{aligned} \quad (1)$$

where $x(t) \in \mathbf{R}^n$ is the state vector in which both rigid and flexible variables are considered, $u(t) \in \mathbf{R}^m$ is the control signal, $y(t) \in \mathbf{R}^l$ is the controlled output, $w_g(t) \in \mathbf{R}^m$ is the gust signal. $A \in \mathbf{R}^{n \times n}$ is the state matrix, $B \in \mathbf{R}^{n \times m}$ is the control matrix, $C \in \mathbf{R}^{l \times n}$ is the output matrix, $B_g \in \mathbf{R}^{n \times m}$ is the input gust matrix and $D_g \in \mathbf{R}^{l \times m}$ is the output gust matrix. This complete aeroservoelastic model is obtained joining two sub-models: (i) the flight dynamic model, that describes the rigid body motion of the aircraft and (ii) the aeroelastic model, which is responsible of the aircraft aeroelasticity. Hypothesis of small disturbances from a steady flight condition allows to linearize the rigid body equations of motion [13] and to uncouple the longitudinal plane response from the lateral one. The rigid state variables are

the longitudinal component of the total airspeed u , the angle of attack α , the pitch angle θ and the pitch rate q . The control variables are the elevator deflection δ_e and the aileron deflection δ_a (divided in outboard deflection $\delta_{a,ou}$ and inboard deflection $\delta_{a,in}$). For both devices only symmetric deflection are evaluated.

The mass and the elastic properties of the aircraft are given by a beam model made in Nastran and the flexible formulation can be obtained from the classical formulation of equations of motion for multi degree of freedom systems, as in

$$M\ddot{x}(t) + C_k\dot{x}(t) + Kx(t) = F(t), \quad (2)$$

where M is the mass matrix, C_k is the viscous damping matrix and K is the stiffness matrix. The flexible vector $x(t)$ is the general time-varying displacement vector and $F(t)$ can be divided into two terms, one related to the aerodynamic components induced by the structural normal modes and the second related to external forces that may not be depending on aerodynamics.

The external aerodynamic force is modelled considering unsteady aerodynamics and is introduced in the statespace model (Eq. 1) using Pade' interpolation method [14]. The aerodynamic forces F_t and the gust forces F_g can be modeled as

$$\begin{aligned} F_t(s) &= \frac{1}{2}\rho V_{tas}^2 FGT(s)\delta(s) \\ F_g(s) &= \frac{1}{2}\rho V_{tas}^2 FGM(s)w(s) \end{aligned} \quad (3)$$

where V_{tas} is the aircraft true airspeed, δ_i is the control device deflection ($i = e, a_{ou}, a_{in}$), w is the gust speed, $FGT(s)$ and $FGM(s)$ are large scale improper transfer function matrices of the particular forms

$$\begin{aligned} FGT(s) &= F_{t0} + F_{t1s} + F_{t2s} s^2 + \sum_{i=1}^N F_{i+2} \frac{s}{s + \sigma_i} \\ FGM(s) &= F_{g0} + F_{g1s} + F_{g2s} s^2 + \sum_{i=1}^N F_{gi+2} \frac{s}{s + \sigma_{gi}} \end{aligned} \quad (4)$$

with F_* and σ_* are intervening coefficient matrices and filter poles from FEM analysis [15].

Time domain aeroelastic analysis is performed to generate responses to active control and/or to external force systems. Gust input causes a variation

of the system aerodynamics that is simulated in state space formulation using the Doublet-Lattice Method ([16]). Panel incidence induced by the gust is computed for each control point of the aerodynamic mesh, that has to be introduced in the model in terms of x, y and z coordinates. The generation of the induced angle of attack due to the gust profile ($F_{gust_j}(t)$) for each aerodynamic control point is expressed in Eq. 5 (discrete gust "1 - cosine" model for a reference system with z upward and x backward),

$$F_{gust_j}(t) = \frac{U}{2U_\infty} \cos(\gamma_j) \left[1 - \cos\left(2\pi f_g \left(t - \frac{x_0 - x_j}{U_\infty}\right)\right) \right] \quad (5)$$

where U is the vertical gust speed, $U_\infty = V_{tas}$ is the aircraft airspeed, $\cos(\gamma_j)$ is the dihedral cosine of each panel control point and f_g is the gust frequency. The distance between the aircraft reference system center and the gust is defined as $x_0 = d_g U_\infty$, with $d_g = 0.1$ s gust time delay. The variable x_j is the x coordinate of the j^{th} aerodynamic control point.

The gust dynamic loads have been calculated by means of the mode displacement (MD) method, which recovers the loads directly from the modal displacements. The MD approach assumes that the modal superposition assumption, used to construct the generalized aeroelastic equations of motion, can also be used to recover the load distributions. Since gust excitation cases are characterized by fairly well-distributed loads, the MD method can be successfully used to calculate the actual loads with a sufficient number of modes. The modal superposition assumption is:

$$\xi(x, t) = \phi(x)\eta(t)$$

where $\phi(x)$ is the matrix of modal displacements and $\eta(t)$ is the vector of natural modes in the range of 1 to 50 Hz of frequency. This assumption implies that the aerodynamic and inertial modal load (forces and moments), integrated for obtaining section loads, can be expressed as:

$$F(x, t) = C_{LOAD}\eta(t) \quad (6)$$

where C_{LOAD} is the integrated stiffness matrix expressed in modal form.

3. Model of Actuator Systems

The simulation model includes two different actuators: (i) one related to the elevator surface (for the pitch rate control) and (ii) one related to the aileron deflection (for the angle of attack variation). For the elevator control surface, an Electro-Mechanical Actuator (EMA) is implemented and is composed of a variable speed bi-directional electric motor coupled with mechanical gears to provide speed reduction and torque amplification. The implemented model is a 2^{nd} order under-damped transfer function with higher bandwidth, due to the gust load alleviation application. No backlash or stiffness variable with external loads is considered. The model is not linear due to:

- the presence of saturations on the input command and on the output surface position. The saturation on the output limits the surface position in a given range and simulates the mechanical stops for the actuator/surface stroke.
- the presence of a rate limiter that simulates a physical limitation in actuator speed.
- the introduction of a computational delay that simulates the transfer time related to flight control computer (FCC) clock.

For the aileron surface, an Electro-HydroStatic Actuator (EHSA) is considered and it contains the following nonlinearities:

- input command saturation and computational delay,
- rate saturation and output surface position saturation (implemented inside the control loop).

For the validation of the control laws, the maximum elevator rate is imposed equal to 60 deg/s and the maximum aileron rate is imposed equal to 80 deg/s. An higher rate is chosen for the aileron surface because it is the device chosen for the gust alleviation (symmetric deflection).

4. \mathcal{L}_1 Adaptive Controller

The choice of the \mathcal{L}_1 adaptive controller for the feedback aircraft control is motivated by the high level of model uncertainty (by the variations of the mass and flight conditions) and by high oscillations in the model responses (by state- and

time-dependent nonlinearities). This controller is composed by three main blocks: (i) the adaptive law, (ii) the state predictor, and (iii) the control law. See Fig. 1 for the detailed architecture.

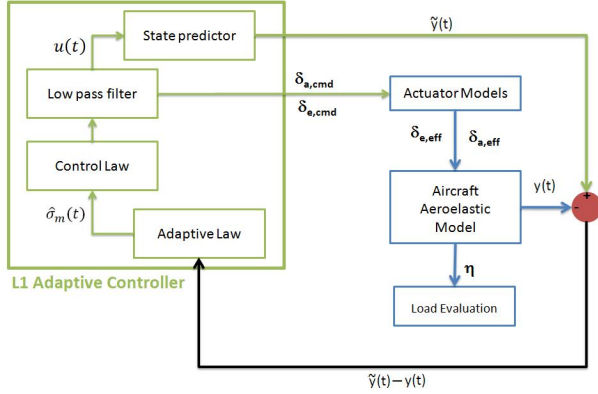


Fig. 1. \mathcal{L}_1 controller architecture

The adaptive law is a piecewise constant law, as explained in Chapter 3.3 of [17] and in [18], that guarantees fast estimation, and the adaptation rate can be associated with the sampling rate of the onboard CPU, equal to 100 Hz. Moreover, this adaptive algorithm guarantees bounded inputs and outputs, uniform transient response and steady-state tracking. This extension of the \mathcal{L}_1 controller was applied to NASA's AirSTAR ([19]) and to the Boeing X-48B ([20]).

The state predictor, which is designed to reproduce the actual plant structure and to specify the desired behavior of the closed-loop system, generates a prediction of the system state. An important feature of the \mathcal{L}_1 controller is that the error between the closed loop system with the \mathcal{L}_1 controller and the reference controller can be uniformly bounded by a constant proportional to the adaptation sampling rate.

Another important key aspect is that this controller defines the control signal as the output of a low-pass filter to guarantee that the control signal stays in the low-frequency range. The low-pass filter for this application is designed with a mixed deterministic and randomized approach as described in [21].

The above described controller is designed to control the general linear system of Eq. (1) which, considering uncertainties, can be rewritten as

$$\begin{aligned} \dot{x}(t) &= A_m x(t) + B_m(\omega u(t) + f_1(x(t), z(t), t)) \\ &\quad + B_{um} f_2(x(t), z(t), t), \quad x(0) = x_0, \\ z(t) &= g_o(x_z(t), t), \quad \dot{x}_z(t) = g(x_z(t), \\ &\quad x(t), t), \quad x_z(0) = x_{z0}, \\ y(t) &= Cx(t). \end{aligned} \quad (7)$$

The matrix $A_m \in R^{n \times n}$ is Hurwitz and specifies the desired dynamics of the closed-loop system, $B_m \in R^{n \times m}$ and $C \in R^{m \times n}$ are known constant matrices. $B_{um} \in R^{n \times (n-m)}$ is a constant matrix such that $B_m^T B_{um} = 0$ and the rank of $B = [B_m \ B_{um}]$ is n . Compared to system (1), the system (7) includes $\omega \in R^{m \times m}$ the unknown frequency gain matrix, $z(t)$ and $x_z(t)$ respectively the output and state vector of internal unmodeled dynamics and the unknown nonlinear functions $g(\cdot)$ and $g_o(\cdot)$.

The state predictor is defined as

$$\begin{aligned} \dot{\hat{x}}(t) &= A_m \hat{x}(t) + B_m(\omega_0 u(t) + \hat{\sigma}_1(t)) + B_{um} \hat{\sigma}_2(t), \\ \hat{x}(0) &= x_0 \end{aligned}$$

where the adaptive vectors $\hat{\sigma}_1(t) \in R^m$ and $\hat{\sigma}_2(t) \in R^{n-m}$, with ω_0 a candidate nominal frequency, are

$$\begin{bmatrix} \hat{\sigma}_1(t) \\ \hat{\sigma}_2(t) \end{bmatrix} = - \begin{bmatrix} \mathbb{I}_m & 0 \\ 0 & \mathbb{I}_{n-m} \end{bmatrix} B^{-1} \Phi^{-1}(T_s) \mu(iT_s), \quad (8)$$

for $i = 0, 1, 2, \dots$, and $t \in [iT_s, (i+1)T_s]$, where $T_s > 0$ is the adaptation sampling time associated with the sampling rate of the FCS computer. In Equation (8) also appear

$$\begin{aligned} \Phi(T_s) &= A_m^{-1}(e^{A_m T_s} - \mathbb{I}_n), \in R^{n \times n} \\ \mu(iT_s) &= e^{A_m iT_s} \tilde{x}(iT_s), \end{aligned}$$

where $\tilde{x}(t) = \hat{x}(t) - x(t)$ is the error between the system state and the predicted state.

Finally, calling s the complex argument resulting from the Laplace transform of the corresponding time domain signal, the last element of the controller is the control law defined as

$$u(t) = -KD(s)\hat{\eta}(s).$$

We also define

$$\begin{aligned} \hat{\eta}(t) &= \omega_0 u(t) + \hat{\eta}_1(t) + \hat{\eta}_{2m}(t) - r_g(t), \\ \hat{\eta}_1(t) &= \hat{\sigma}_1(t), \\ \hat{\eta}_{2m}(s) &= H_m^{-1}(s) H_{um}(s) \hat{\sigma}_2(s), \\ r_g(s) &= K_g(s) r(s) \end{aligned}$$

where $D(s)$ is a proper stable transfer matrix of dimension $m \times m$, $r(t)$ is the reference signal. The transfer functions H_m and H_{um} are calculated starting from the matrices of systems (7)

$$H_m(s) = C(s\mathbb{I}_n - A_m)^{-1}B_m$$

$$H_{um}(s) = C(s\mathbb{I}_n - A_m)^{-1}B_{um}$$

while the prefilter $Kg(s)$ is chosen as the constant matrix $K_g = -(CA_m^{-1}B_m)^{-1}$ to achieve decoupling among the signals.

A matched Multi-Input Multi-Output (MIMO) \mathcal{L}_1 controller is implemented in which the input controls are the elevator and aileron deflections. The angle of attack α at the IMU station and the pitch rate q are the matched controlled variables.

Even if a complete rigid-flexible model is considered, the controller state predictor reproduces only the rigid dynamics and the flexible components are indirectly controlled by these variables. The scope of this simplified design is to verify whether or not the overall system can be controlled by using the rigid states of the aircraft [8].

5. Simulation Results

The aircraft state vector has both rigid and flexible components, related to the aircraft longitudinal plane. Twentytwo natural modes η_i in the range of frequency 1 to 50 Hz and one Pade' term for the definition of unsteady aerodynamic coefficients are considered. The sampling rate of the feedback adaptive controller is equal to 100 Hz. The input controls are the elevator and splitted aileron symmetric deflections.

As controlled variables for gust alleviation the dynamic loads in the wing root working station have to be reduced to guarantee the controller efficiency, even when uncertainties occur (i.e. variation of the mass, flight conditions and gust frequency). Thus, the vertical force and the moments around X and Y axes are analyzed, as the loads are directly evaluated from the natural modes (Eq. 6). The aircraft characteristics are reported in Table I. For the nominal configuration Zero Fuel Weight (ZFW) is considered as the reference mass (equal to 50540 kg as in Table I) and the 1st symmetric bending mode ($f_g = 3.41$ Hz) are considered as reference conditions.

Different cases are analyzed:

TABLE I
AIRCRAFT CHARACTERISTICS AND FLIGHT CONDITIONS

Mass	m = 50540 kg
Mean Aerodynamic Chord	c = 3.746 m
Wing span	b = 34.14 m
Vertical true airspeed at sea level	$V_{tas} = 163.34$ m/s
Mach number	M = 0.48
Gust frequency (1 st bending mode)	$f_g = 3.41$ Hz

- 1) variation of the aileron rate speed to take into account physical limitations of the actuator models,
- 2) variation of the mass and flight conditions to evaluate the robustness of the controller in presence of model uncertainties (no retuning of the controller parameters),
- 3) variations of gust frequency to prove the controller adaptation at difference disturbance inputs.

For the first case three aileron maximum rate are considered: (i) 60 deg/s, (ii) 80 deg/s and (iii) 100 deg/s. The closed loop case of an ideal actuator model with an aileron rate limiter at 100 deg/s and a saturation limiter at ± 15 deg is also considered.

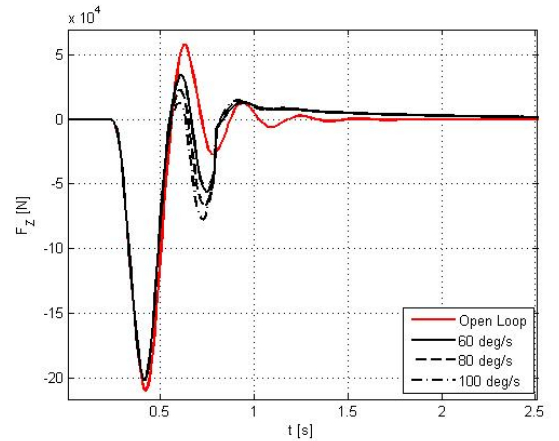


Fig. 2. Variation of the vertical force with different aileron rate limiter

As in Figs.2-4 and in Table II, even if an aileron speed limiter is implemented, good performance are obtained: a reduction of about 5% of the vertical force and of about 10 – 18% for the moment variations are obtained.

As visible in Figs. 5-7, a reduction of the vertical

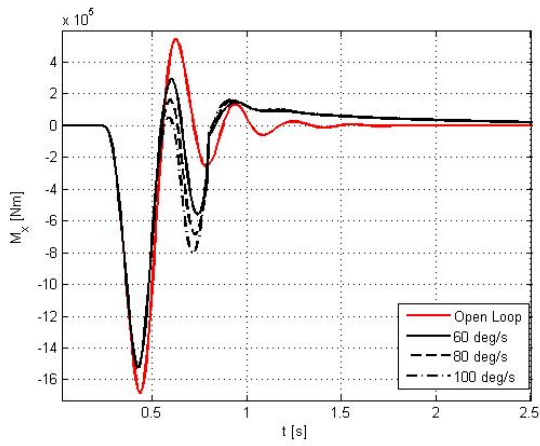


Fig. 3. Variation of the moment around X axis with different aileron rate limiter

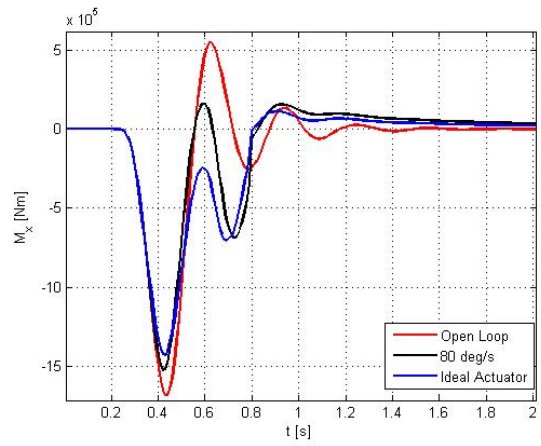


Fig. 6. Variation of the moment around X axis with a real and ideal actuator

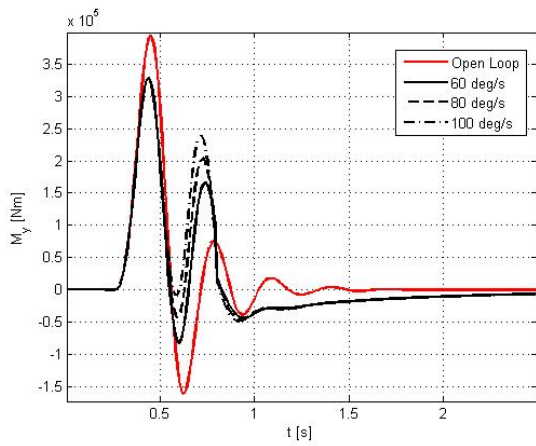


Fig. 4. Variation of the moment around Y axis with different aileron rate limiter

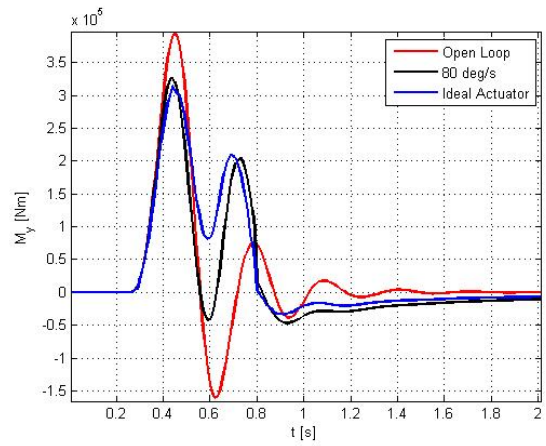


Fig. 7. Variation of the moment around X axis with a real and ideal actuator

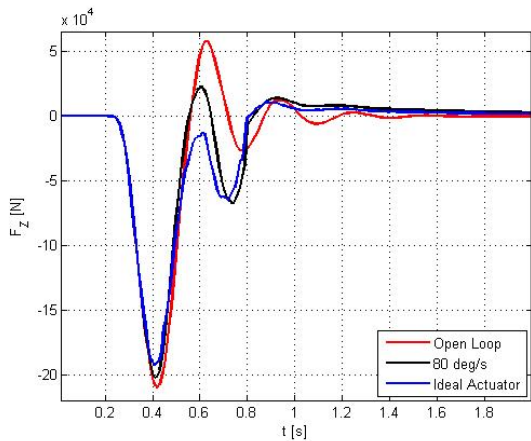


Fig. 5. Variation of the vertical force with a real and ideal actuator

force F_z of 10% is obtained with an ideal actuator, even considering a limitation on the aileron rate

TABLE II

OPEN AND CLOSED LOOP RESPONSES: IDEAL AND REAL ACTUATORS

Real Actuator			
Open Loop	$F_z = -2.103 \cdot 10^5$	$M_x = -1.683 \cdot 10^6$	$M_x = 3.936 \cdot 10^5$
Real Actuator			
Closed loop 60 deg/s	$F_z = -2.022 \cdot 10^5$	$M_x = -1.526 \cdot 10^6$	$M_x = 3.283 \cdot 10^5$
Real Actuator			
Closed loop 80 deg/s	$F_z = -2.021 \cdot 10^5$	$M_x = -1.523 \cdot 10^6$	$M_x = 3.267 \cdot 10^5$
Real Actuator			
Closed loop 100 deg/s	$F_z = -2.021 \cdot 10^5$	$M_x = -1.523 \cdot 10^6$	$M_x = 3.267 \cdot 10^5$
Ideal Actuator	$F_z = -1.912 \cdot 10^5$	$M_x = -1.432 \cdot 10^6$	$M_x = 3.145 \cdot 10^5$

and a saturation limit. Better results are obtained for the moments around X and Y axes: more than 20% of reduction is obtained. No computational delay is considered for the ideal case.

Considering the results obtained with the aileron rate variation, a limiter at $80deg/s$ is considered for all the other cases.

For the second case variations of $\pm 40\%$ of the state matrix are analyzed. These parameter variations can be caused by change on the considered reference airspeed, on the mass configuration, on the aerodynamic derivatives, . . . The variations are considered with a percentage reduction or augmentation of the state matrix elements. This validation is performed to verify that a retuning of the controller parameters are not necessary if a substantial variation is considered. The MTOW condition is not analyzed because the mass variation with respect to the ZFW configuration is about 10%. For classical robust controller, a small oscillation of the matrix parameters is allowed without changing the controller parameters.

Classical robust controllers (as LQR controller) require a retuning of the weight parameters if the model is uncertain. Different approaches can be considered in presence of uncertainties, as probabilistic and randomized [22], [23] or LMI approaches [24].

If \mathcal{L}_1 adaptive controller is implemented, the adaptation law permits to follow the desired responses without loss of robustness, because in this particular adaptive controller the adaptation is separated to the robustness (as explained in [17]).

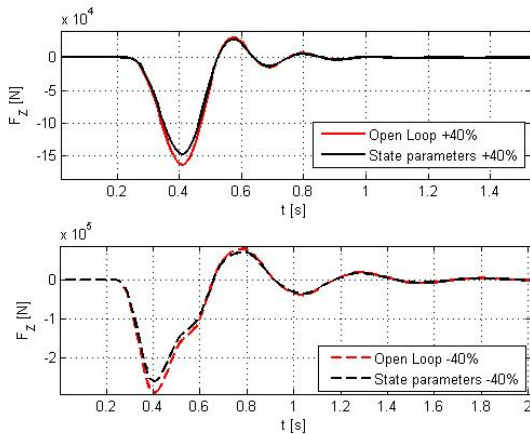


Fig. 8. Variation of the vertical force with state parameter changes

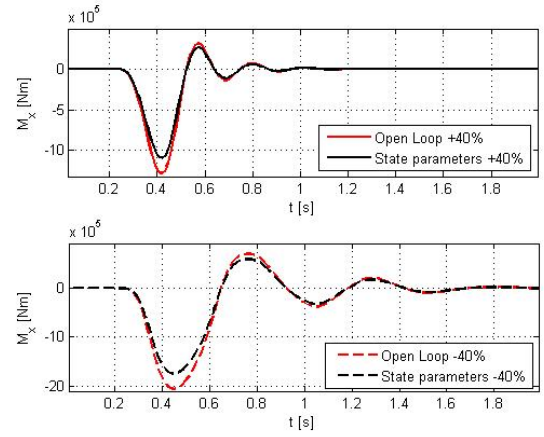


Fig. 9. Variation of the moment around X axis with state parameter changes

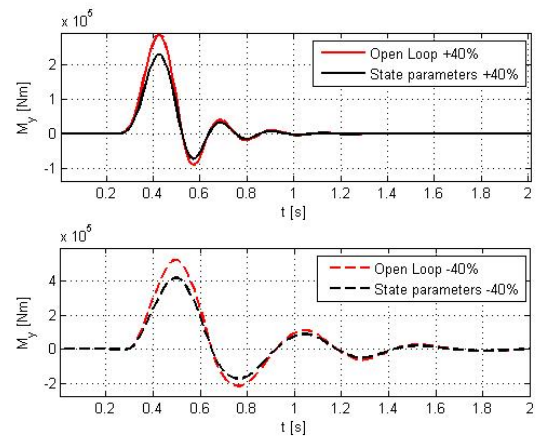


Fig. 10. Variation of the moment around X axis with state parameter changes

In Figs.8-10 the load variation at the wing root are considered, when the state matrix parameters are changed. The open loop simulation with the changed matrices is also performed. As visible, the maximum (absolute) peak of the vertical force is reduced of about 10% and of about 20% for the moments. See Table III for detailed results.

For the third case a *quasi static* input (as a slow maneuver) is analyzed. Usually, if the controller parameters are tuned for a dynamic gust, a retuning of the controller could be required for slower gust inputs. In this case no changes are required for the controller parameters.

In Figs. 11-13 a slow gust frequency ($1.74Hz$) is considered for the ZFW condition and in Figs. 14-16 a slow gust for the MTOW condition. In

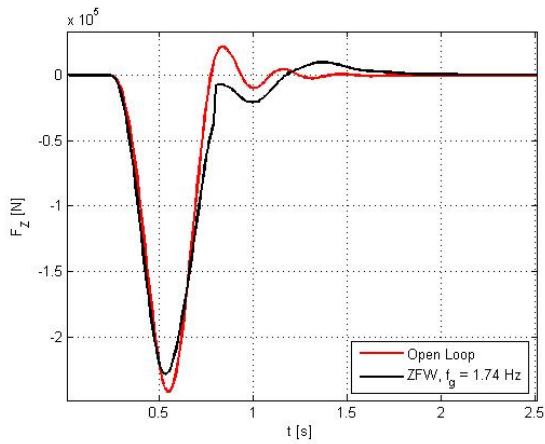


Fig. 11. Variation of the vertical force for a gust of 1.74 Hz (ZFW)

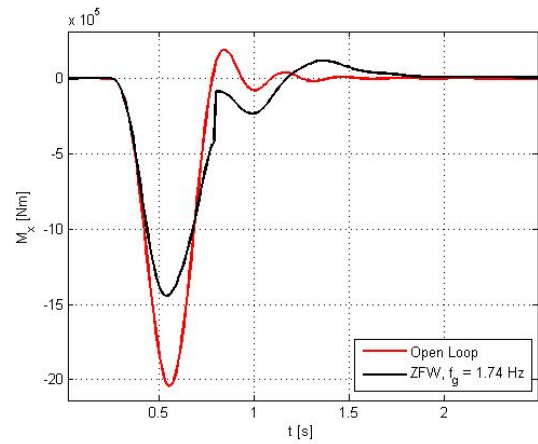


Fig. 12. Variation of the moment around X axis for a gust of 1.74 Hz (ZFW)

both cases a reduction of about 10 – 35% can be observed in the load variations. See Table IV for detailed results.

6. Conclusions

An adaptive controller for gust load alleviation is considered and preliminary evaluation of the controller robustness in presence of uncertainties is performed. The results are obtained with a sampling rate of 100 Hz and an aileron rate limiter at 80deg/s. Good controller performance (alleviation of about 20% of the wing loads) is proved for different mass and flight condition

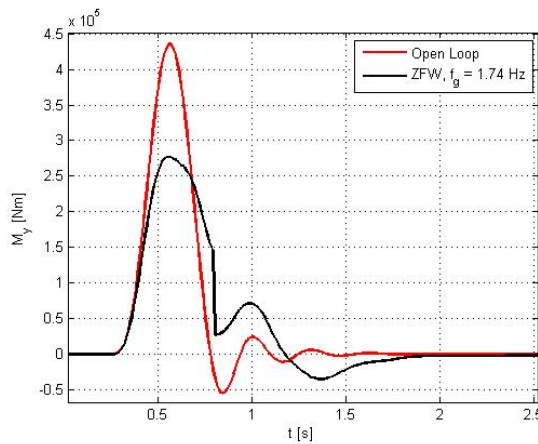


Fig. 13. Variation of the moment around Y axis for a gust of 1.74 Hz (ZFW)

TABLE III

OPEN AND CLOSED LOOP RESPONSES: VARIATIONS OF THE SYSTEM PARAMETERS

Real Actuator			
Open Loop			
Variations of +40%			
$F_z = -1.619 \cdot 10^5$	$M_x = -1.284 \cdot 10^6$	$M_x = 2.872 \cdot 10^5$	
Real Actuator			
Closed loop 80 deg/s			
Variations of +40%			
$F_z = -1.475 \cdot 10^5$	$M_x = -1.091 \cdot 10^6$	$M_x = 2.297 \cdot 10^5$	
Real Actuator			
Open Loop			
Variations of -40%			
$F_z = -2.889 \cdot 10^5$	$M_x = -2.056 \cdot 10^6$	$M_x = 5.196 \cdot 10^5$	
Real Actuator			
Closed loop 80 deg/s			
Variations of -40%			
$F_z = -2.61 \cdot 10^5$	$M_x = -1.747 \cdot 10^6$	$M_x = 4.146 \cdot 10^5$	

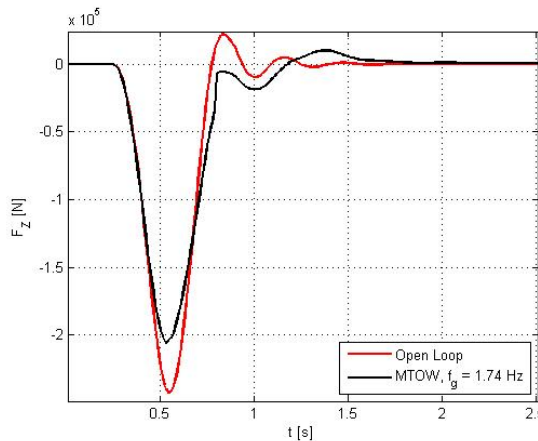


Fig. 14. Variation of the vertical force for a gust of 1.74 Hz (MTOW)

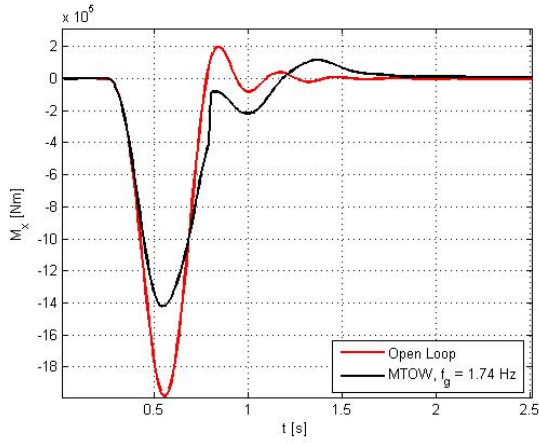


Fig. 15. Variation of the moment around X axis for a gust of 1.74 Hz (MTOW)

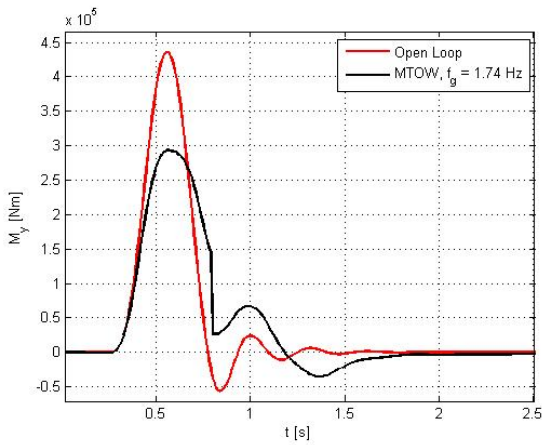


Fig. 16. Variation of the moment around Y axis for a gust of 1.74 Hz (MTOW)

configurations. The complete system (controller and aircraft model) is also validated for a 'quasi static' gust input, to verify that a rigid predictor enforces alleviation of loads without requiring gain scheduling. Future works will be the integration of the flexible model, associating a Proportional Integrative Derivative controller with the 1 adaptive controller and the evaluation of the wing loads. The combination of PID controller and adaptive controller should improve the performance of the adaptive controller, reducing the first peak of the flexible variables (as explained in [25]). To improve the reduction of the loads, a feedforward controller will be considered, starting from the measurement of a probe sensor in the vehicle nose.

TABLE IV

OPEN AND CLOSED LOOP RESPONSES: VARIATION OF THE GUST FREQUENCY, $f_g = 1.74Hz$

Real Actuator			
Open Loop, ZFW	$F_z = -2.421 \cdot 10^5$	$M_x = -2.039 \cdot 10^6$	$M_x = 4.356 \cdot 10^5$
Real Actuator			
Closed loop, ZFW	$F_z = -2.281 \cdot 10^5$	$M_x = -1.444 \cdot 10^6$	$M_x = 2.754 \cdot 10^5$
Real Actuator			
Open Loop, MTOW	$F_z = -2.419 \cdot 10^5$	$M_x = -1.981 \cdot 10^6$	$M_x = 4.36 \cdot 10^5$
Real Actuator			
Closed loop, MTOW	$F_z = -2.056 \cdot 10^5$	$M_x = -1.42 \cdot 10^6$	$M_x = 2.935 \cdot 10^5$

Copyright Statement

The authors confirm that they, and/or their company or organization, hold copyright on all of the original material included in this paper. The authors also confirm that they have obtained permission, from the copyright holder of any third party material included in this paper, to publish it as part of their paper. The authors confirm that they give permission, or have obtained permission from the copyright holder of this paper, for the publication and distribution of this paper as part of the ICAS 2014 proceedings or as individual off-prints from the proceedings.

REFERENCES

- [1] M. Alam, *Gust Load Alleviation System for BWB (Blended Wing Body) Flexible Aircraft*, Czech Technical University, PhD. Dissertation, 2013.
- [2] M.J. Dillsaver, C.E.S. Cesnik and I.V. Kolmanovsky, "Gust Load Alleviation Control for Very Flexible Aircraft," *AIAA Atmospheric Flight Mechanics Conference*, Portland, USA, 2011.
- [3] S. Haghghat, H.H.T. Liu and J.R.R.A. Martins, "Model-Predictive Gust Load Alleviation Controller for a Highly Flexible Aircraft," *Journal of Guidance, Control, and Dynamics*, vol. 35(6), pp. 1751-1766, 2012.
- [4] N. Aouf, B. Boulet and R. Botez, "Robust Gust Load Alleviation for a Flexible Aircraft," *Canadian Aeronautics and Space Journal*, vol. 46, pp. 131-139, 2000.

- [5] N. Jansson and D. Eller, "Robust Turbulence Load Alleviation," *IFASD 2011: International Forum on Aeroelasticity and Structural Dynamics*, Paris, France, 2011.
- [6] N. Aouf, B. Boulet and R. Botez, "H2 and H-inf Optimal Gust Load Alleviation for a Flexible Aircraft," *Proceedings of the American Control Conference*, Chicago, USA, 2000.
- [7] N. Aouf and B. Boulet, "Uncertainty-based model-order reduction of flexible systems preserving robust closed-loop performance," *Proceedings of the Institution of Mechanical Engineers, Part G: Journal of Aerospace Engineering*, 2008, vol. 222 (2), pp. 291-295.
- [8] G. Avanzini, E. Capello, I. Piacenza, F. Quagliotti, E. Xargay and N. Hovakimyan, " \mathcal{L}_1 Adaptive Control of Flexible Aircraft: Preliminary Results," *AIAA Atmospheric Flight Mechanics Conference*, Toronto, Canada, 2010.
- [9] E. Capello, G. Guglieri and F. Quagliotti, "A Comprehensive Robust Adaptive Controller for Gust Load Alleviation," *The Scientific World Journal*, vol. 2014, 12 pages, 2014, doi:10.1155/2014/609027
- [10] A. Wildschek and R. Maier, "Integrated Adaptive Feed-forward Control of Atmospheric Turbulence excited Rigid Body Motions and Structural Vibrations on a Large Transport Aircraft," *American Control Conference*, Seattle, USA, 2008.
- [11] J. Zeng, B. Moulin, R. de Callafon and M.J. Brenner, "Adaptive Feedforward Control for Gust Load Alleviation," *Journal of Guidance, Control, and Dynamics*, vol. 33(3), pp. 862872, 2010.
- [12] A. Wildschek, *An Adaptive Feed-Forward Controller for Active Wing Bending Vibration Alleviation on Large Transport Aircraft*, Technische Universität München, PhD. Dissertation, 2008.
- [13] B. Etkin and L. Reid, *Dynamics of Flight: Stability and Control*, New York: John Wiley and Sons, 1996.
- [14] G.A. Baker Jr. and P. Graves-Morris, *Pade' Approximants*, Cambridge U.P., 1996.
- [15] G. Puyou and Y. Lossier, "Clearance Benchmark for a Civil Aircraft," in *Optimization based clearance of flight control laws*, Lecture Notes in Control and Information Sciences, vol. 416, pp. 11-36, 2012.
- [16] W.P. Rodden, "The Development of the Doublet-Lattice Method," *International Forum on Aeroelasticity and Structural Dynamics*, Rome, June 1997.
- [17] N. Hovakimyan and C. Cao, *\mathcal{L}_1 Adaptive Control Theory*, Philadelphia: Society for Industrial and Applied Mathematics, 2010.
- [18] E. Xargay, N. Hovakimyan and C. Cao, " \mathcal{L}_1 Adaptive Controller for Multi-Input Multi-Output Systems in the presence of nonlinear unmatched uncertainties," *Proceedings of American Control Conference*, pp. 875-879, 2010.
- [19] N. Hovakimyan, C. Cao, E. Kharisov and E. Xargay, \mathcal{L}_1 Adaptive Control for Safety-critical Systems, *IEEE Control Systems Magazine*, vol. 31(5), pp. 54-104, 2011.
- [20] T. Leman, E. Xargay, G. Dullerud and N. Hovakimyan, " \mathcal{L}_1 Adaptive Control Augmentation System for the X-48B Aircraft," *AIAA Guidance, Navigation and Control Conference*, Chicago, USA, 2009.
- [21] E. Capello, F. Quagliotti and R. Tempo, "Randomized Approaches for Control of QuadRotor UAVs," *Journal of Intelligent and Robotic Systems*, vol. 73, pp. 157-173, 2014.
- [22] Q. Wang and R.F. Stengel, "Robust control of nonlinear systems with parametric uncertainty," *Automatica*, vol. 38, pp. 1591-1599, 2002.
- [23] B.T. Polyak and R. Tempo, "Probabilistic Robust Design with Linear Quadratic Regulators," *Systems and Control Letters*, vol. 43, pp. 343-353, 2001.
- [24] E. Jeung, D. Oh, J. Kim, and H. Park, H., "Robust Controller Design for Uncertain Systems with Time Delays: LMI Approach," *Automatica*, vol. 32, pp. 1229-1231, 1996.
- [25] E. Capello, D. Sartori, G. Guglieri and F. Quagliotti, "Design and validation of an \mathcal{L}_1 adaptive controller for mini-UAV autopilot," *Journal of Intelligent and Robotic Systems*, vol. 69, pp. 109-118, 2013.